UDC 539.17

MODELING AND OPTIMIZATION OF THE ANGULAR DISTRIBUTION MEASUREMENT FOR THE ^{10}B(*n,d*)^{9}Be REACTION AT THE NG-150 NEUTRON GENERATOR

Ruziev Elbek Tulkinovich,
National University of Uzbekistan
named after M.Ulugbek,
Senior Lecturer at Institute of Nuclear
Physics AS RU, Senior Researcher, PhD
ruziev@inp.uz

Abstract. *This work details the modeling and geometric optimization of angular distribution measurements for the $^{10}B(n,d)^{9}Be$ reaction conducted with a laboratory neutron generator and a ΔE-E silicon telescope. The primary goal was to establish an optimal experimental window that ensures clean separation between the ^{9}Be ground and excited states while minimizing measurement time. A mathematical model for the total full width at half maximum (FWHM) was derived by combining detector resolution, target energy straggling, and angular-geometric broadening factors. Our simulation results identify the precise target thicknesses and detector distances needed to prevent peak distortion. The proposed methodology enhances both spectral resolution and counting throughput, providing practical guidelines for executing highly efficient differential cross-section experiments under restricted laboratory conditions.*

Keywords: *(n,d) nuclear reactions, scattering kinematics, NG-150 generator, silicon detector array, full width at half maximum (FWHM), energy resolution, peak separation.*

МОДЕЛИРОВАНИЕ И ОПТИМИЗАЦИЯ ИЗМЕРЕНИЯ УГЛОВОГО РАСПРЕДЕЛЕНИЯ ДЛЯ РЕАКЦИИ ^{10}B(*n,d*)^{9}Be НА НЕЙТРОННОМ ГЕНЕРАТОРЕ НГ-150

Аннотация. *В данной работе подробно описаны моделирование и геометрическая оптимизация измерений углового распределения для реакции $^{10}B(n,d)^{9}Be$, проведённых с использованием лабораторного нейтронного генератора и $\Delta E - E$ кремниевого телескопа. Основная цель заключалась в установлении оптимального экспериментального окна, обеспечивающего чёткое разделение основного и возбуждённых состояний ядра ^{9}Be при минимизации времени измерений. Математическая модель для полной ширины на полувысоте (FWHM) была получена путём объединения разрешения детектора, страгглинга энергии в мишени и угловых геометрических факторов уширения. Результаты моделирования определяют точные толщины мишеней и расстояния до детекторов, необходимые для предотвращения искажения пиков. Предложенная методология повышает как спектральное разрешение, так и скорость счёта, предоставляя практические рекомендации для проведения высокоэффективных экспериментов по дифференциальному сечению в ограниченных лабораторных условиях.*

Ключевые слова: *(n,d) ядерные реакции, кинематика рассеяния, генератор НГ-150, кремниевая детекторная система, полная ширина на полувысоте (FWHM), энергетическое разрешение, разделение пиков.*

NG-150 NEYTRON GENERATORIDA ^{10}B(*n,d*)^{9}Be REAKSIYASI UCHUN BURCHAK TAQSIMOTINI O‘LCHASHNI MODELLASHTIRISH VA OPTIMALLASHTIRISH

Annotatsiya. *Ushbu ishda laboratoriya neytron generatori hamda $\Delta E - E$ kremniy teleskopi yordamida o‘tkazilgan $^{10}B(n,d)^{9}Be$ reaksiyasining burchak taqsimoti o‘lchovlarini modellashtirish va geometrik optimallashtirish tafsilotlari keltirilgan. Asosiy maqsad o‘lchash vaqtini kamaytirish bilan birga, ^{9}Be yadrosining asosiy va uyg‘otilgan holatlarini aniq ajratishni ta’minlaydigan optimal eksperimental sharoitni belgilashdan iborat edi. Umumiy yarim kenglik (FWHM) uchun matematik model detektor rezolyutsiyasi, nishondagi energiya stragglingi hamda burchak-geometrik kengayish omillarini birlashtirish orqali ishlab chiqildi. Simulyatsiya natijalarimiz spektral cho‘qqilarning buzilishini oldini olish uchun zarur bo‘lgan nishon qalinligi va detektorgacha bo‘lgan masofalarni aniq belgilab berdi. Taklif etilayotgan metodologiya spektral rezolyutsiya va sanoq samaradorligini oshirib, cheklangan laboratoriya sharoitida yuqori effektivlikka ega differensial kesim eksperimentlarini o‘tkazish bo'yicha amaliy tavsiyalar beradi.*

Kalit so'zlar: *(n,d) yadro reaksiyalari, sochilish kinematikasi, NG-150 generatori, kremniy detektorlar sistemasi, yarim kenglik (FWHM), energiya rezolyutsiyasi, cho'qqilarni ajratish.*

Introduction. Neutron-induced (*n,d*) nuclear reactions serve as a cornerstone for both fundamental nuclear physics and practical fields like radiation dosimetry, material analysis, and neutron diagnostics [1]. Reactions tracking boron isotopes are of particular significance due to their substantial cross-sections at low energy thresholds and their widespread utilization in modern neutron detection systems. Specifically, investigating the ^{10}B(*n,d*)^{9}Be reaction yields critical insights into underlying reaction mechanisms and angular distributions, both of which are essential for refining computational models of neutron-matter interactions.

While laboratory-scale neutron generators offer an accessible alternative [1,6] and operationally straightforward alternative for differential cross-section measurements, they introduce notable experimental constraints. Neutrons generated via deuteron-induced reactions are inherently non-monoenergetic and carry an angular dispersion that directly degrades the energy resolution of outgoing charged particles. Furthermore, the finite geometry of both targets and detectors induces additional spectral broadening. These combined factors frequently culminate in peak overlap, severely complicating the isolation of closely spaced reaction channels, such as the ground and first excited states of the residual ^{9}Be nucleus.

In standard Δ*E*–*E* silicon telescope configurations [2,4,7], the overall energy resolution is governed by a combination of independent physical mechanisms: intrinsic detector noise, energy straggling within the boron target, primary neutron beam dispersion, and geometric solid-angle acceptance. Poor management of these components leads to distorted particle identification and prolonged acquisition times due to low signal-to-background ratios. Long measurement cycles are highly undesirable as they exacerbate electronic drift, beam fluctuations, and background accumulation. Thus, establishing an analytical optimization framework before executing the experiment is essential to balance data-taking speed with adequate spectral resolution.

Although numerical modeling has previously been used to forecast spectral distortion, systematic studies that unify resolution modeling, explicit peak separation thresholds, and beam-time efficiency for the ^{10}B(*n,d*)^{9}Be process remain remarkably scarce [5]. Furthermore, the interplay between two-body kinematics and detector positioning has not been adequately explored for experiments localized at the NG-150 neutron generator facility.

The present work addresses this gap by establishing a comprehensive, multi-component energy resolution model. The total full width at half maximum (FWHM) is evaluated via the quadratic summation of all individual broadening sources. Using these criteria, we evaluate the precise conditions under which adjacent ^{9}Be states can be cleanly resolved. It is important to emphasize that this paper does not present raw experimental data; rather, it provides a comprehensive theoretical feasibility study utilizing kinematic calculations and LISE++ assisted modeling to deliver practical, optimized guidelines for upcoming laboratory cross-section campaigns [3].

Experimental Concept and Reaction Kinematics. The configured experimental framework is engineered to efficiently generate fast neutrons, induce the (*n,d*) reaction within the boron matrix, and record the trajectory of emitted deuterons with superior energy resolution. The operational core of this configuration relies on the following sub-systems: Deuterons are accelerated to an energy of 100 keV using the NG-150 facility to bombard a titanium–tritium (TiT) target. Through the standard T(*d,n*)^{4}He reaction dynamic, fast neutrons are extracted. Due to the geometric constraints and energy variations within the tritium layer, these neutrons span a finite energy spread rather than being strictly monoenergetic. The neutrons are directed onto a thin ^{10}B target, where the (*n,d*) reaction occurs. The thickness of the boron target is optimized to achieve a balance between reaction yield and minimization of energy straggling effects. The emitted deuterons are detected using a Δ*E*–*E* silicon telescope system. The thin Δ*E* detector measures the initial energy loss of the particle, while the thicker E detector measures the residual energy, enabling accurate particle identification and precise energy determination. The detectors are positioned at specific laboratory scattering angles to measure the angular distribution of emitted deuterons. The distance between the boron target and the detector active area defines the solid angle, which affects both counting statistics and energy resolution.

Figure 1 illustrates the schematic configuration of the experimental setup. The experiment is performed using the NG-150 neutron generator, in which neutrons are produced in a TiT production target. The generated neutrons interact with a thin ^{10}B boron target, where the ^{10}B(*n,d*)^{9}Be reaction occurs. In this study, neutrons emitted at laboratory angles close to 90° with respect to the incident deuteron beam are used, since this region provides a relatively narrow neutron energy distribution, i.e., a more quasi-monoenergetic neutron beam.

The emitted deuterons are detected using a Δ*E*-*E* silicon telescope system positioned at predetermined laboratory scattering angles. The detector placement is defined by the target-to-detector distance L and the detector active diameter D, which together determine the solid-angle coverage, affecting both counting statistics and the overall energy resolution of the measurement.

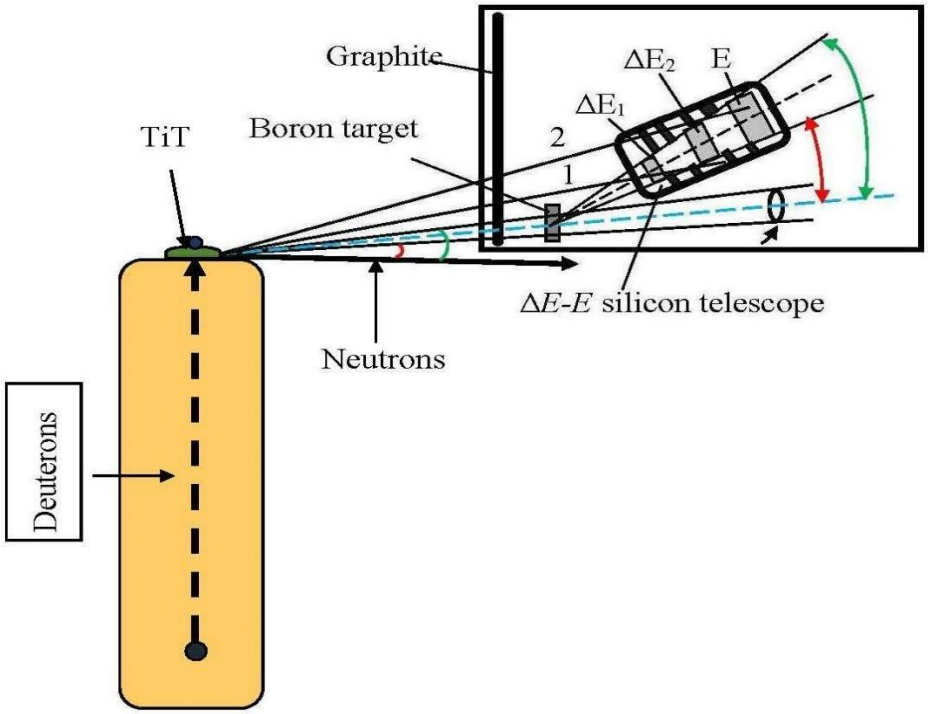


Figure 1. Schematic representation of the experimental setup used for the measurement of the ^{10}B(*n*,*d*)^{9}Be reaction, showing the NG-150 neutron generator, the TiT neutron production target, the ^{10}B target, and the Δ*E*-*E* silicon telescope.

Modeling of Energy Resolution. The accurate measurement of the differential cross-section for the ^{10}B(*n*,*d*)^{9}Be reaction strongly depends on the energy resolution of the detection system. The total energy resolution of the Δ*E*-*E* telescope is determined by several independent contributions combined in quadrature:

$$FWHM_{tot} = \sqrt{FWHM_{det}^2 + FWHM_{str}^2 + FWHM_{n,\theta}^2 + FWHM_{\theta_d}^2} \quad (1)$$

where $FWHM_{det}^2$ is the intrinsic detector resolution, $FWHM_{str}^2$ energy straggling in target material, $FWHM_{n,\theta}^2$ accounts for the energy spread from neutron angular distribution, $FWHM_{\theta_d}^2$ represents broadening caused by detector geometry and solid angle.

Detector Resolution Contribution ($FWHM_{det}^2$). The intrinsic energy resolution of the silicon detectors is mainly determined by electronic noise and statistical fluctuations in the charge collection process. The detector contribution to the energy resolution can be characterized by the full width at half maximum ($FWHM_{det}$) of the spectral peaks.

To determine the intrinsic detector resolution, Gaussian fitting was applied to five well-resolved peaks in the ^{226}Ra alpha spectrum using Origin software, as illustrated in Figure 2. The $FWHM_{det}$ values obtained from the individual peaks were initially determined in channel units.

Subsequently, an energy calibration was performed using a linear calibration function relating channel number to energy. Using this calibration, the $FWHM_{det}$ values were converted from channels to energy units (keV). The average value of the converted $FWHM_{det}$ values was then used to estimate the intrinsic energy resolution of the detector.

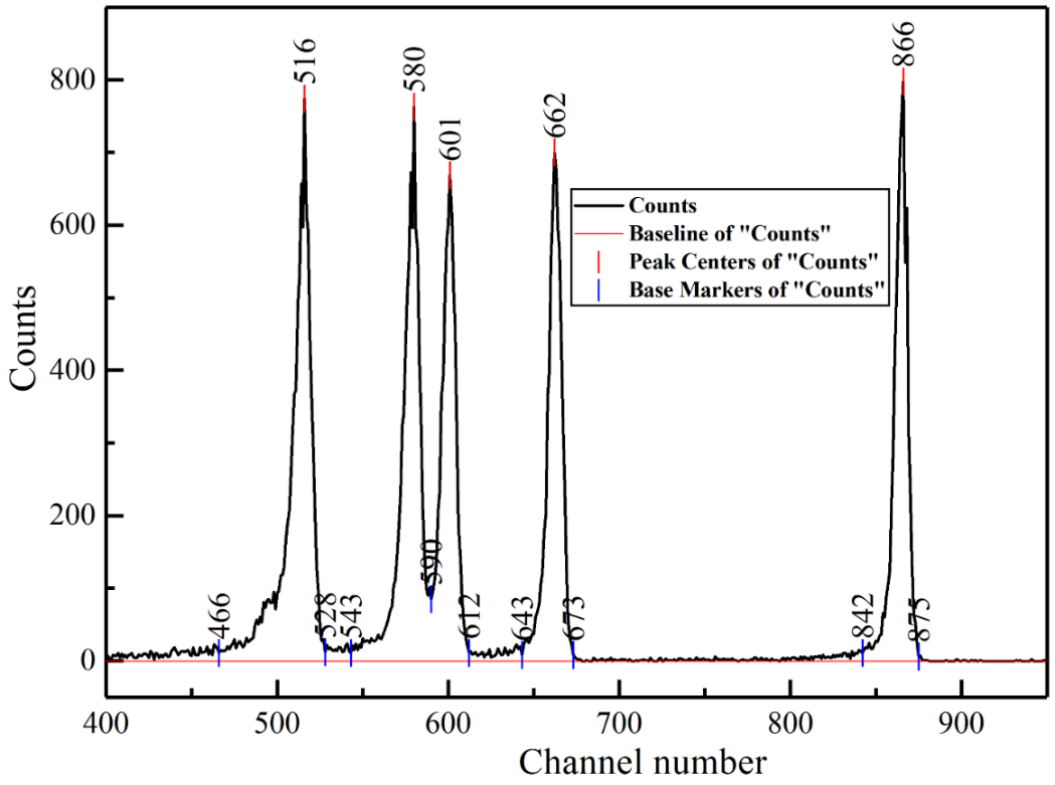


Figure 2. Vacuum spectrum of the ^{226}Ra source measured using the silicon *E*-detector. The peak used for intrinsic resolution determination is shown with Gaussian fitting.

Target Energy Straggling ($FWHM_{str}^2$). The target energy straggling contribution arises from statistical fluctuations in energy loss as deuterons traverse the boron target material. The straggling width was evaluated using stopping power calculations implemented in simulation packages such as LISE++, taking into account target thickness, material density, and particle transport effects [3,8]. The energy straggling contribution was obtained numerically using Monte Carlo based stopping power simulations. As deuterons traverse the boron target, they experience multiple small-angle collisions with target atoms, leading to statistical fluctuations in energy loss, known as energy straggling. The contribution of energy straggling to the total energy resolution can be expressed as:

$$FWHM_{str} = 2.355 \cdot \sigma_{str} \quad (2)$$

Where σ_{str} is typically obtained from simulation software such as LISE++. In this work, the straggling contribution was determined using simulation-based stopping power calculations. The energy loss and straggling parameters were evaluated using nuclear interaction simulation tools such as **LISE++**, which provide numerical estimates of particle energy distribution inside the boron target.

The dependence of the mean deuteron energy loss and the corresponding energy broadening in terms of $FWHM_{str}$ on the boron target thickness was evaluated using SRIM-based simulations. As shown in Figure 3, both the average energy loss and the spectral broadening increase with increasing target thickness. While a thicker target improves reaction yield, it also significantly degrades the spectral resolution due to enhanced energy straggling. Therefore, an optimal target thickness was selected to ensure a balance between sufficient counting statistics and acceptable energy resolution for the Δ*E*-*E* telescope measurements. Increasing target thickness enhances reaction yield but leads to additional spectral broadening. The selected thickness represents a compromise between counting statistics and energy resolution.

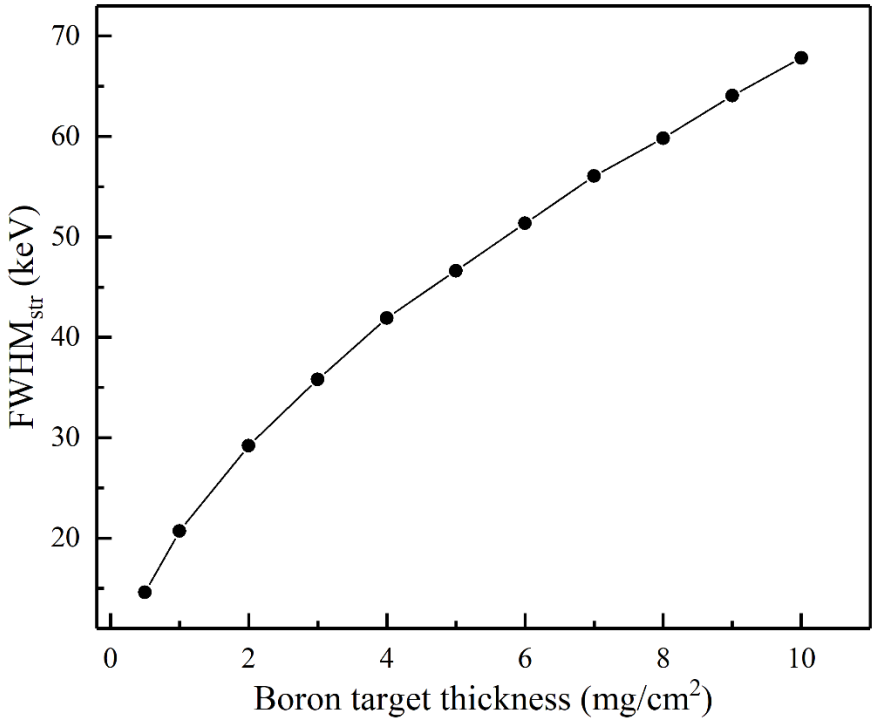


Figure 3. Simulated mean energy loss and energy broadening (expressed as $FWHM_{str}$) of deuterons in the boron target as a function of target thickness.

Neutron Angular Spread Contribution ($FWHM^2_{n,\theta}$). Neutrons produced in the TiT production target of the NG-150 generator are emitted with a finite energy and angular distribution due to the intrinsic deuteron beam energy spread and the geometrical thickness of the tritium target. As a consequence, the incident neutron energy at the boron target is not strictly monoenergetic. Since the detected deuteron energy depends on the neutron energy through reaction kinematics,

$$E_d = f(E_n, \theta_{lab}) \quad (3)$$

variations in neutron energy lead directly to a spread in the measured deuteron energy at a fixed laboratory angle [9]. The corresponding contribution to the energy resolution can be evaluated using standard error propagation:

$$\mathrm{FWHM_{n,\theta}} = \left|\frac{\partial \mathrm{E_d}}{\partial \mathrm{E_n}}\right| \cdot \mathrm{FWHM_{E_n}} \quad (4)$$

$\mathrm{FWHM_{E_n}}$ is the neutron energy spread and $\frac{\partial \mathrm{E_d}}{\partial \mathrm{E_n}}$ represents the kinematic sensitivity factor calculated at the selected laboratory angle. The derivative $\frac{\partial \mathrm{E_d}}{\partial \mathrm{E_n}}$ was determined numerically from reaction kinematics by varying the neutron energy around its nominal value and evaluating the corresponding change in deuteron energy at each measurement angle. The neutron energy distribution was obtained from the known kinematics of neutron production in the TiT target and the specified deuteron beam energy spread of the NG-150 generator. The neutron angular spread contribution was evaluated using reaction kinematics. The sensitivity of the detected deuteron energy to neutron energy variation was estimated as the derivative $\frac{\partial \mathrm{E_d}}{\partial \mathrm{E_n}}$, and the neutron energy spread $\mathrm{FWHM_{E_n}}$ was calculated analytically without relying on pre-tabulated simulation data.

The neutron energy is expressed as a function of the incident deuteron energy and neutron emission angle:

$$E_n = f(E_d, \theta_n) \quad (5)$$

where E_d is the deuteron beam energy, and $\theta_n$is the neutron emission angle in the laboratory frame.

The neutron energy resolution contribution was evaluated using the error propagation method. The corresponding full width at half maximum is given by:

$$FWHM^2_{E_n} = \left(\frac{\partial E_n}{\partial E_d}\right)^2 \cdot \left(FWHM^2_{beam} + FWHM^2_{str,T}\right) + \left(\frac{\partial E_n}{\partial \theta_n}\right)^2 \cdot (\Delta\theta_n)^2 \quad (6)$$

Beam energy and target straggling term: $FWHM^2_{beam} + FWHM^2_{str,T}$ represents the effective deuteron energy spread arising from accelerator beam energy dispersion and energy straggling inside the titanium–tritium target. $FWHM^2_{beam} = 2.355 \cdot \sigma_{beam}$, $FWHM^2_{str,T} = 2.355 \cdot \sigma_{str,T}$

Kinematic sensitivity factor: $\left(\frac{\partial E_n}{\partial E_d}\right)$ describes the dependence of neutron energy on the incident deuteron energy based on reaction kinematics.

Angular dispersion contribution: $\frac{\partial E_n}{\partial \theta_n}$ accounts for neutron energy variation due to angular emission distribution. $\Delta\theta_n$ represents the angular acceptance range determined by the production target geometry. The neutron energy resolution contribution was calculated analytically without relying on pre-tabulated simulation data, ensuring transparency of the modeling procedure.

To quantify the neutron angular spread contribution, the reaction kinematics of the ^{10}B(n,d)^{9}Be process was evaluated. The dependence of the detected deuteron energy on the incident neutron energy was calculated analytically, and the sensitivity factor $\frac{\partial E_d}{\partial E_n}$ was determined at each laboratory angle.

As shown in Figure 4, the deuteron energy varies nearly linearly with the incident neutron energy in the energy range relevant for the NG-150 generator. The relationship is illustrated for several laboratory scattering angles: 0°, 15°, 30°, 45°, and 60°. The slope of each curve corresponds to the kinematic amplification factor, which defines how the neutron energy broadening propagates into the measured deuteron spectrum and is used in calculating the $FWHM_{n,\theta}$ contribution.

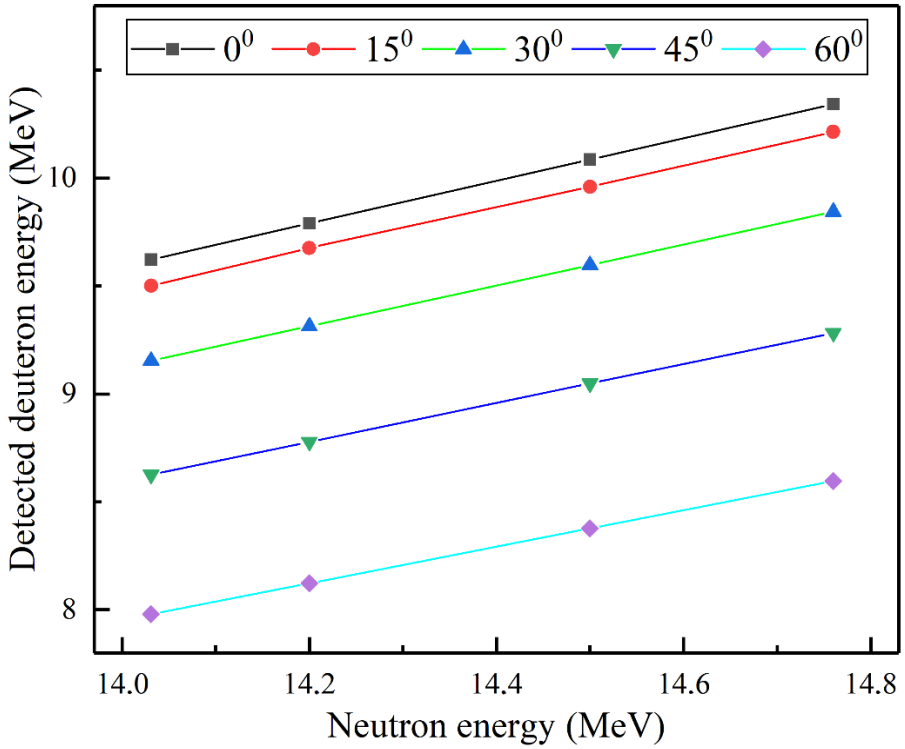


Figure 4. Deuteron energy as a function of incident neutron energy for the ^{10}B(n,d)^{9}Be reaction at different laboratory scattering angles (0°, 15°, 30°, 45°, and 60°).

Detector Solid Angle Contribution ($FWHM^2_{\theta_d}$). Even if the incident neutron beam were perfectly collimated and monoenergetic, the finite size of the detector introduces an additional source of energy broadening. Because the detector subtends a finite solid angle, particles emitted within a small angular interval $\Delta\theta_d$ are detected simultaneously. Since the reaction kinematics depends on the laboratory angle, this angular acceptance results in a spread of detected deuteron energies.

The corresponding contribution to the total energy resolution is obtained by propagating the angular uncertainty through the reaction kinematics:

$$FWHM_{\theta_d} = \left|\frac{\partial E_d}{\partial \theta_d}\right| \cdot \Delta\theta_d \quad (7)$$

Determination of angular acceptance. For a circular detector of active diameter D placed at a distance L from the target, the angular acceptance can be approximated as:

$$\Delta\theta_d \approx 2\arctan\left(\frac{D}{2L}\right) \quad (8)$$

Where, D is the detector active diameter, and L is the target-to-detector distance.

The influence of detector angular acceptance on the measured energy resolution was evaluated using reaction kinematics. Because the detector subtends a finite angular interval $\Delta\theta_d$, particles emitted at slightly different laboratory angles are recorded simultaneously. Since the deuteron energy depends on emission angle, this effect introduces additional spectral broadening.

The influence of the detector solid angle on the measured energy resolution was evaluated for a detector of active diameter D = 1 cm at various target-to-detector distances (L = 10, 20, 30, 40, 50, and 60 cm). As shown in Figure 5, the geometrical broadening contribution ($FWHM_{\theta_d}$) decreases with increasing L, while the effect becomes more pronounced at larger laboratory scattering angles due to kinematic sensitivity. These results provide guidance for optimizing detector placement to minimize angular broadening without compromising counting statistics.

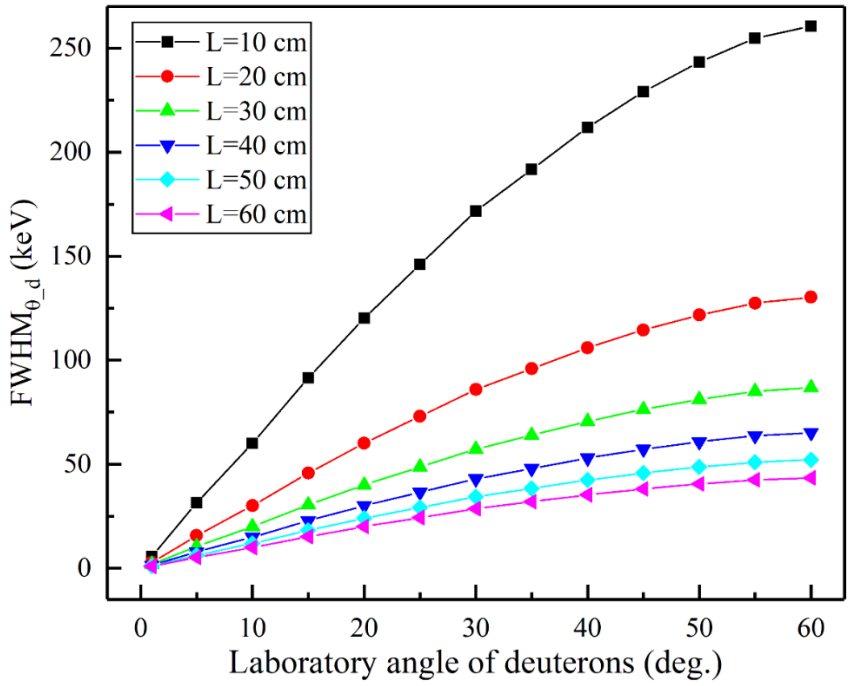


Figure 5. Contribution of the detector solid angle ($FWHM_{\theta_d}$) to the total energy resolution as a function of laboratory scattering angle for a detector of diameter D = 1 cm at various target-to-detector distances (L = 10, 20, 30, 40, 50, and 60 cm).

Total Resolution and Optimization. The total energy resolution obtained by combining all independent contributions can be used to evaluate the separation of reaction peaks corresponding to the ground and excited states of ^{9}Be. To ensure reliable peak discrimination, a commonly adopted separation criterion requires that the distance between adjacent peaks be at least $1.5 \cdot FWHM_{tot}$ [11].

Based on the resolution model developed in this work, the following experimental parameters were optimized: Boron target thickness, Detector-target distance and detector active area, Laboratory observation angles.

Through analytical modeling, these parameters can be adjusted to achieve minimal spectral broadening while preserving sufficient counting statistics for reliable measurement. The proposed optimization framework provides a practical approach for improving energy resolution and measurement efficiency in differential cross section studies using neutron generator based experimental systems.

The total energy resolution ($FWHM_{tot}$) was evaluated by combining all independent contributions, including intrinsic detector resolution, target energy straggling, neutron angular spread, and detector solid angle effects. For Figure 6, calculations were performed assuming a boron target thickness of 20 μm and a target-to-detector distance of L = 12 cm. The results show that the total FWHM exhibits a clear angular dependence due to kinematic sensitivity and geometric broadening, with better spectral resolution at forward angles compared to larger scattering angles. This provides guidance for selecting optimal detector placement and target parameters to ensure reliable peak separation of the ^{9}Be ground and excited states.

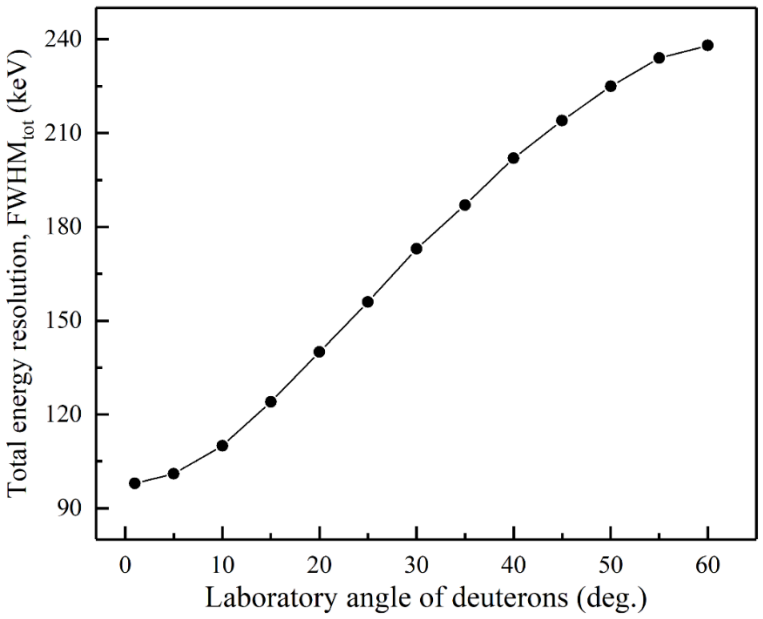


Figure 6. Total energy resolution ($FWHM_{tot}$) as a function of laboratory scattering angle for the ^{10}B(n,d)^{9}Be reaction.

Peak Separation Criteria and Optimization. Accurate separation of the ^{9}Be ground and excited state peaks is essential for reliable differential cross section measurements of the ^{10}B(n,d)^{9}Be reaction. The energy levels of the ^{9}Be residual nucleus, including the ground state and first few excited states, were obtained from evaluated nuclear data [10], which provide excitation energies and corresponding deuteron group energies used in peak identification (see evaluated nuclear level compilations). To ensure sufficient resolution of adjacent states, a commonly adopted separation criterion is:

$$|E_1 - E_2| > 1.5 \cdot FWHM_{tot} \quad (9)$$

where E_1 and E_2 are the deuteron energies associated with the ground and first excited states of ^{9}Be, respectively, and $FWHM_{tot}$ is the total energy resolution defined in Section 3. The fulfillment of this criterion strongly depends on observation angle, target thickness, and detector geometry. Therefore, systematic parameter variation was performed to identify the optimal experimental region. This criterion helps prevent artificial overlap of peaks in the measured spectrum and thus reduces systematic errors in cross section extraction.

Several key experimental parameters influence the ability to meet this peak separation criterion and must be carefully optimized:

While thicker targets increase reaction yield, they also enhance energy straggling, which broadens peaks. Conversely, thinner targets reduce straggling but may lead to lower counting statistics.

Increasing the distance between the target and detector reduces geometric broadening ($FWHM_{\theta_d}$) by decreasing the angular acceptance. However, this also reduces the solid angle and, therefore, the count rate. Due to two-body reaction kinematics, certain laboratory angles provide larger separation between deuteron energy peaks corresponding to different ^{9}Be states. Modeling using kinematic relations or simulation tools such as LISE++ can help identify optimal angles for detector placement [3].

By adjusting these parameters according to the separation criterion, the total FWHM can be minimized while ensuring that the ground and excited state peaks remain resolvable. Optimization of these factors also contributes to reducing the total measurement time without compromising energy resolution or statistical accuracy. The developed resolution model was applied to evaluate the expected experimental performance for the ^{10}B(n,d)^{9}Be reaction under realistic geometric and target conditions.

Individual broadening contributions, including intrinsic detector resolution, target straggling, neutron angular spread, and detector solid angle effects, were calculated for representative laboratory angles and target thicknesses. The total energy resolution was obtained by quadratic summation of these independent terms. The present study represents a theoretical evaluation of the expected experimental performance for the ^{10}B(n,d)^{9}Be reaction using a compact neutron generator. The results are based on kinematic calculations and LISE++ simulations aimed at assessing peak separation capability prior to experimental implementation [3].

For typical experimental parameters, the dominant contributions arise from target energy straggling and intrinsic detector resolution, while geometrical effects become significant at larger laboratory angles. For

the optimized configuration, the separation condition $|E_1 - E_2| > 1.5 \cdot FWHM_{tot}$ is satisfied across a broad range of laboratory angles. The separation margin decreases for thicker targets due to increased straggling but improves at forward angles where kinematic sensitivity is reduced.

The modeling results suggest the following practical recommendations: Select boron target thickness to balance reaction yield and energy straggling. Position detectors at laboratory angles that maximize peak separation according to two-body kinematics. Increase detector distance where feasible to reduce geometrical broadening while maintaining acceptable count rates. These findings demonstrate that careful analytical modeling enables optimization of spectral quality while minimizing total measurement time.

Conclusion. In this work, a comprehensive analytical model for the total energy resolution of the Δ*E*-*E* detection system was developed and applied to the ^{10}B(*n*,*d*)^{9}Be reaction using a neutron generator. All major broadening mechanisms including intrinsic detector resolution, energy straggling in the boron target, neutron angular spread, and detector geometrical acceptance—were systematically evaluated.

The combined resolution model enabled quantitative prediction of peak separation between the ground and first excited states of ^{9}Be. By applying a well-defined separation criterion, optimal experimental parameters were identified, including boron target thickness, detector distance, and laboratory observation angles, ensuring reliable peak discrimination while maintaining sufficient counting statistics.

The results demonstrate that careful modeling of resolution contributions allows efficient optimization of experimental conditions, leading to improved spectral quality and reduced acquisition time. This methodology provides a practical framework for differential cross section measurements using neutron generator-based systems and can be extended to other neutron-induced charged-particle reactions. The study defines a realistic parameter window in which separation of the ^{9}Be ground and excited states becomes experimentally feasible using compact neutron generator facilities.

Acknowledgements. "This work was supported by the Ministry of Higher Education, Science and Innovations of the Republic of Uzbekistan (Grant No. FL-9024094149, *"Study of nucleon or cluster transfer nuclear reactions to solve problems in nuclear astrophysics and thermonuclear reactions"*)."

REFERENCES:

1. Generatory Neytronov. Metod izmereniya potoka bystrykh neytronov [Neutron Generators. Method for Measuring Fast Neutron Flux]. GOST 22751-77, IPK Izdatel'stvo Standartov, Moscow, USSR, 1977. (in Russian)

2. Artemov, S. V., et al. "Metody izmereniy spektrov bystrykh neytronov na neytronnom generatore NG-150 IYaF AN RUz" [Methods for measuring fast neutron spectra at the NG-150 neutron generator of INP AS RU]. Vestnik Molodykh Uchenykh [Bulletin of Young Scientists], pp. 27–31, 2019. (in Russian)

3. Tarasov, O. B., and Bazin, D. "LISE++: Radioactive beam production with in-flight separators." Nuclear Instruments and Methods in Physics Research Section B: Beam Interactions with Materials and Atoms, vol. 266, no. 19-20, pp. 4657–4664, 2008.

4. Artemov, S. V., et al. "Method for measuring the energy of fast neutrons by the recoil deuterons using a telescope of semiconductor Si detectors." Proceedings of the II International Scientific Forum "Nuclear Science and Technologies", Almaty, Kazakhstan, June 24–27, 2017, pp. 213–214.

5. Aripov, G. A., Kurbanov, B. I., and Zinovyev, V. G. "Opredeleniye soderzhaniya azota i bora metodom spektrometrii gamma-izlucheniya zakhvata neytronov" [Determination of nitrogen and boron content by neutron-capture gamma-ray spectrometry]. Gornyy Vestnik Uzbekistana [Mining Bulletin of Uzbekistan], no. 28, issue 1, p. 102, 2007. (in Russian)

6. Valkovic, V. Neutron Generators for Technical Applications. CRC Press, 2016.

7. Knoll, G. F. Radiation Detection and Measurement. 4th ed., John Wiley & Sons, 2010.

8. Ziegler, J. F., Ziegler, M. D., and Biersack, J. P. "SRIM – The stopping and range of ions in matter." Nuclear Instruments and Methods in Physics Research Section B, vol. 268, no. 11-12, pp. 1818-1823, 2010.

9. Marion, J. B., and Young, F. C. Nuclear Reaction Analysis: Graphs and Tables. North-Holland Publishing Company, 1968.

10.Brown, D. A., et al. "ENDF/B-VIII.0: The 8^{th} Major Release of the Nuclear Reaction Data Library with ENDF/B-VIII.0." Nuclear Data Sheets, vol. 148, pp. 1-142, 2018.

11.Leo, W. R. Techniques for Nuclear and Particle Physics Experiments. 2nd ed., Springer-Verlag, 1994.